Journal of Solution Chemistry, Vol. 24, No. 9, 1995

Apparent Molar Volumes of Aqueous Calcium Chloride to 250°C, 400 bars, and from Molalities of 0.242 to 6.150

Charles S. Oakes,[1] John M. Simonson,[2] * and Robert J. Bodnar[1]

Received August 30, 1993; Revised June 8, 1995

Relative densities of $CaCl_2(aq)$ with $0.242 \leq m/(mol\text{-}kg^{-1}) \leq 6.150$ were measured with vibrating- tube densimeters between 25 and 250°C and near 70 and 400 bars. Apparent molar volumes V_ϕ calculated from the measured density differences were represented with the Pitzer ion-interaction treatment, with appropriate expressions chosen for the temperature and pressure dependence of the virial coefficients of the model. It was found that the partial molar volume at infinite dilution V_ϕ^o, and the second and third virial coefficients B^V and C^V, were necessary to represent V_ϕ near the estimated experimental uncertainty. The ionic-strength dependent $\beta^{(1)v}$ term in the B^V coefficient was included in the fit. The representation for V_ϕ has been integrated with respect to pressure to establish the pressure dependence of excess free energies over the temperature range studied. The volumetric data indicate that the logarithm of the mean ionic activity coefficient, ln $\gamma_\pm(CaCl_2)$, increases by a maximum of 0.3 at 400 bars, 250°C, and 6 $mol\text{-}kg^{-1}$ as compared with its value at saturation pressure.

KEY WORDS: Thermodynamics; density; calcium chloride; high temperature; pressure effects.

[1]Department of Geological Sciences, Virginia Polytechnic Institute and State University, Blacksburg, VA 24061. Current address: Department of Chemistry, Univ. of California, Berkeley, CA 94720.

[2]Chemistry Division, Oak Ridge National Laboratory, Oak Ridge, TN 37831

0095-9782/95/0900-0897$07.50/0 © 1995 Plenum Publishing Corporation

1. INTRODUCTION

This paper continues our series of reports[1,2] on the volumetric properties of aqueous NaCl and $CaCl_2$ solutions at elevated pressures and temperatures and from about 0.2 mol-kg^{-1} to near saturation at ambient temperature. Relative densities of $CaCl_2$(aq) were measured at 25 to 250°C and near 70 and 400 bars using vibrating-tube densimeters at Oak Ridge National Laboratory. Apparent molar volumes (V_ϕ) were calculated from the measured relative densities and as with the previous studies[1,2] the data have been fitted with a pressure and temperature dependent form of the Pitzer ion-interaction model.[3] The equations representing V_ϕ presented in this paper are valid to 250°C, pressures between the saturation vapor pressure and 400 bars, and molalities up to 6.150 mol-kg^{-1}. This represents experimental measurements over a significantly wider range of temperatures, pressures, and molalities than previously available.

In comparison with NaCl, relatively few studies of the density of $CaCl_2$(aq) have been carried out at elevated temperatures and pressures. Of the available measurements (c.f. references in Monnin[4,5]), the results of Gates and Wood[6,7] span the widest range of temperature, pressure, and molality, extending to 325°C, 400 bars, and 6.424 mol-kg^{-1}. Comparisons with a selected subset[6-13] of the published $CaCl_2$(aq) volumetric measurements are made using the model equation based on the present results to calculate V_ϕ's remote to our experimental pressures and temperatures.

The molality-independent fit coefficients have been integrated with respect to pressure to yield differences in activity coefficients $\ln[\gamma_\pm(p)/\gamma_\pm(p_o)]$ relative to values at the saturation vapor pressure (p_o). These values may be used in conjunction with published ion-interaction fits of mean ionic activity coefficients along the vapor-saturation surface to determine activity coefficients for $CaCl_2$(aq) to 400 bars, 250°C, and 6 mol-kg^{-1}.

2. EXPERIMENTAL PROCEDURE

Two $CaCl_2$(aq) stock-solutions, 6.150 and 1.499 m (mol-kg^{-1}), were prepared from $CaCl_2 \cdot 2H_2O$ (EM Science) and distilled, deionized H_2O. The molality of the concentrated solution was determined both by dessication following the procedure described previously[1] and by comparison of measured densities at 25°C and 1 bar and calculating the molality from the correlation equation given by Oakes *et al.*[14] These two independent methods gave analyses in good agreement at m =

6.150±0.005. The 1.499 mol-kg^{-1} stock-solution was prepared by mass dilution of the 6.150 solution, with appropriate correction to masses in vacuum.

The apparent molar volumes V_ϕ reported here were obtained from density differences ($\delta\rho$) between the solution of interest and water using two different high-pressure vibrating-tube densimeters. The design and construction of the densimeters have been described in a previous communication.[2] These results were obtained contemporaneously with our measurements on NaCl(aq);[2] the tube calibration was the same as those used in the NaCl(aq) study, based on H_2O-D_2O, H_2O-NaCl(aq), and H_2O-Ar pairs of known-density fluids at experimental temperatures and pressures.

3. DATA AND CORRELATION OF RESULTS

Apparent molar volumes (V_ϕ) were calculated from

$$V_\phi = 1000\frac{\rho_o-\rho}{m\rho\rho_o}+\frac{M}{\rho} \qquad (1)$$

where M = 110.986 g-mol^{-1}, m is the $CaCl_2$(aq) molality, and ρ and ρ_o are the densities of the solution and water, respectively. Water densities used for transforming the measured $\delta\rho$ to V_ϕ were calculated from the Haar *et al.*[15] equation of state. The measured V_ϕ at each experimental temperature, pressure, and $CaCl_2$(aq) molality are listed in Table I.

V_ϕ from this study and the 25 and 35°C results of Oakes *et al.*[1] at 1 bar are represented with a temperature and pressure dependent form of the Pitzer ion-interaction model[16] given by

$$V_\phi = V_\phi^o+\nu\,|z_M z_X|\frac{A_V}{2b}\ln(1+b\sqrt{I})+2\nu_M\nu_X mRT[B^V+\nu_M z_M mC^V] \qquad (2)$$

where V_ϕ^o is the partial molar volume of the neutral salt at infinite dilution; A_V is the volumetric Debye-Hückel limiting law slope as defined by Bradley and Pitzer[17] and incorporates the dielectric constant equation of Archer and Wang[18] for water and the equation of state for water of Hill;[19] I is the ionic strength; b = 1.2 kg$^{1/2}$-mol$^{-1/2}$; B^V and C^V are the second and third virial coefficients; and R = 83.144 cm^3-bar-mol^{-1}-K^{-1}. The ionic strength dependence of the second virial coefficient is assumed to be given by

$$B^V = \beta^{(0)V}+\frac{2\beta^{(1)V}}{\alpha^2 I}[1-(1+\alpha\sqrt{I})\exp(-\alpha\sqrt{I})] \qquad (3)$$

Table I. Apparent Molar Volumes, Fit Deviations, Water Densities, and Density Differences for $CaCl_2$(aq)

t °C	p bars	m mol-kg^{-1}	V_ϕ cm^3-mol^{-1}	δV_ϕ	ρ_0[a] g-cm^{-3}	$10^3\delta\rho$
24.97	73.8	6.1500	33.06	0.19	1.00032	398.34
24.96	73.6	4.9574	31.44	0.08	1.00032	341.24
24.96	73.4	3.8404	29.94	0.17	1.00031	279.21
24.95	73.4	2.7919	28.38	0.31	1.00031	213.74
24.96	73.1	1.8058	26.52	0.35	1.00030	145.59
24.95	73.1	0.8768	24.37	0.54	1.00030	74.38
24.96	72.6	1.4990	25.54	0.06	1.00027	123.39
24.96	72.7	1.2414	24.89	0.04	1.00028	103.70
24.96	72.8	0.9869	24.16	0.00	1.00028	83.71
24.96	72.8	0.7356	23.43	0.05	1.00028	63.33
24.96	72.6	0.7356	23.46	0.08	1.00027	63.31
24.94	72.7	0.4874	22.84	0.41	1.00028	42.50
24.96	72.6	0.2422	21.40	0.26	1.00027	21.59
24.89	417.0	6.1500	33.74	0.19	1.01504	395.72
24.89	417.0	4.9518	32.29	-0.08	1.01504	338.23
24.89	417.0	3.8319	30.99	-0.06	1.01504	276.07
24.89	417.0	2.7830	29.59	0.02	1.01504	211.05
24.89	417.0	1.7984	28.09	0.22	1.01504	143.21
24.90	417.0	1.4990	27.12	-0.14	1.01503	121.96
24.90	417.0	1.2408	26.57	-0.10	1.01503	102.39
24.90	417.0	0.9860	26.02	-0.01	1.01503	82.50
24.90	417.0	0.7346	25.28	-0.01	1.01503	62.45
24.90	417.0	0.4865	24.68	0.28	1.01503	41.93
24.90	417.0	0.2417	24.13	0.95	1.01503	21.10
50.04	71.3	6.1500	33.83	0.10	0.99106	391.43
50.04	71.2	4.9573	32.19	0.09	0.99105	335.50
50.04	70.8	3.8402	30.62	0.14	0.99104	274.88
50.03	70.4	2.7917	28.96	0.17	0.99102	210.78
50.04	70.6	2.7917	28.89	0.10	0.99103	211.00
50.03	70.5	1.8057	27.25	0.30	0.99103	143.30
50.03	70.6	1.4990	26.36	0.08	0.99103	121.32
50.04	71.2	0.8767	24.50	-0.16	0.99105	73.77
50.03	70.5	0.9867	25.07	0.09	0.99103	82.22
50.03	70.3	0.7354	24.37	0.17	0.99102	62.18
50.03	70.4	0.4873	23.58	0.32	0.99102	41.84
50.03	70.6	0.2421	22.62	0.68	0.99103	21.14
50.04	409.0	6.1500	34.54	-0.21	1.00504	388.52
50.04	408.0	4.9516	33.04	-0.29	1.00500	332.43
50.04	407.0	3.8317	31.66	-0.21	1.00496	271.74

Table I. Continued

t °C	p bars	m mol-kg^{-1}	V_ϕ cm^3-mol^{-1}	δV_ϕ	ρ_0[a] g-cm^{-3}	$10^3\delta\rho$
50.03	406.0	2.7827	30.31	-0.02	1.00493	207.60
50.03	407.0	1.7982	28.77	0.14	1.00497	140.99
50.04	408.0	1.4990	27.85	-0.19	1.00500	120.01
50.04	407.0	0.9857	26.77	-0.05	1.00496	81.14
50.04	408.0	0.7344	26.03	-0.07	1.00500	61.43
50.04	407.0	0.4863	25.53	0.31	1.00496	41.19
50.03	406.0	0.2416	25.14	1.15	1.00493	20.69
99.56	72.3	6.1500	33.39	-0.14	0.96202	389.64
99.55	71.7	4.9573	31.39	0.01	0.96200	335.13
99.55	72.0	3.8402	29.35	0.07	0.96202	275.82
99.55	71.7	2.7917	27.24	0.10	0.96200	212.18
99.56	72.0	1.8057	24.72	-0.08	0.96201	145.25
99.56	71.5	0.8767	22.02	0.15	0.96199	74.36
99.56	71.5	1.4990	23.81	-0.13	0.96199	122.80
99.55	71.9	0.9867	22.18	-0.11	0.96201	83.34
99.56	71.4	0.7354	21.37	0.08	0.96198	63.02
99.56	72.2	0.4873	20.29	0.19	0.96202	42.48
99.56	71.0	0.2421	18.25	-0.19	0.96196	21.67
99.55	411.0	6.1500	34.28	0.08	0.97688	386.10
99.56	411.0	4.9516	32.51	0.10	0.97688	331.17
99.55	411.0	2.7827	28.80	0.01	0.97688	208.88
99.55	411.0	1.7982	26.74	0.00	0.97688	142.39
99.56	411.0	0.8723	24.82	0.63	0.97688	72.39
99.56	408.0	1.4990	25.79	-0.21	0.97675	121.05
99.56	409.0	0.9857	24.43	-0.12	0.97679	81.96
99.56	409.0	0.7344	23.76	0.07	0.97679	61.92
99.56	408.0	0.4863	22.74	0.09	0.97675	41.72
99.56	411.0	0.2416	22.12	0.86	0.97688	20.99
149.83	74.0	6.1500	30.85	-0.36	0.92110	398.18
149.83	73.6	4.9573	28.32	-0.07	0.92108	343.29
149.82	73.7	3.8402	25.40	-0.02	0.92109	284.29
149.83	73.7	2.7917	22.00	-0.17	0.92109	220.80
149.82	73.5	1.8057	18.03	-0.38	0.92108	152.41
149.83	71.0	1.4990	17.01	0.02	0.92094	128.58
149.83	71.0	1.4990	16.80	-0.19	0.92094	128.87
149.83	71.0	0.9867	14.21	-0.04	0.92094	87.83
149.82	73.1	0.8767	13.78	0.18	0.92106	78.50
149.82	71.0	0.7354	12.68	0.05	0.92095	66.69

Table I. Continued

t °C	p bars	m mol-kg^{-1}	V_ϕ cm^3-mol^{-1}	δV_ϕ	ρ_0[a] g-cm^{-3}	$10^3\delta\rho$
149.83	71.0	0.4873	10.57	-0.12	0.92094	45.23
149.82	71.0	0.242	18.29	0.19	0.92095	23.00
149.83	414.0	6.1500	32.28	0.27	0.93871	392.65
149.83	415.0	4.9516	30.01	0.16	0.93876	337.84
149.83	415.0	3.8317	27.56	0.13	0.93876	278.56
149.83	414.0	2.7827	24.83	0.16	0.93871	215.09
149.83	414.0	1.7982	21.73	0.29	0.93871	147.51
149.83	413.0	1.4990	20.07	-0.19	0.93866	126.10
149.83	415.0	0.8723	17.97	0.61	0.93876	75.96
149.83	413.0	0.7344	16.48	-0.09	0.93866	65.11
149.83	413.0	0.4863	14.90	-0.10	0.93866	43.98
149.83	413.0	0.2416	12.85	-0.11	0.93866	22.37
199.79	72.6	6.1500	25.88	0.20	0.86927	415.59
199.79	72.2	4.9573	22.42	0.27	0.86924	359.55
199.79	72.3	3.8402	18.12	0.11	0.86925	299.78
199.79	72.0	2.7917	13.02	-0.05	0.86923	234.46
199.79	71.8	2.7917	13.38	0.31	0.86921	233.52
199.80	72.1	1.8057	6.68	-0.24	0.86923	163.38
199.79	71.7	1.4990	4.74	0.20	0.86921	138.39
199.79	72.0	0.9857	-0.29	-0.07	0.86923	95.34
199.79	71.5	0.8767	-0.58	0.84	0.86919	85.00
199.79	71.8	0.7344	-3.18	-0.08	0.86921	72.76
199.79	71.9	0.4863	-7.17	-0.61	0.86922	49.70
199.80	411.0	6.1500	28.33	-0.06	0.89188	406.96
199.80	411.0	4.9516	25.37	-0.39	0.89188	350.92
199.80	410.0	3.8317	21.88	-0.46	0.89182	290.85
199.80	409.0	2.7827	18.03	-0.03	0.89176	225.44
199.80	409.0	1.7982	13.06	0.34	0.89176	156.04
199.80	410.0	1.4990	10.89	0.13	0.89182	133.45
199.79	413.0	0.9857	6.46	-0.41	0.89202	92.00
199.80	411.0	0.8723	5.40	-0.44	0.89188	82.26
199.79	411.0	0.7344	4.37	-0.18	0.89189	69.95
199.79	411.0	0.4863	1.36	-0.57	0.89189	47.59
249.78	72.2	6.1500	16.55	-0.21	0.80314	446.09
249.78	71.6	4.9573	11.59	0.21	0.80308	386.95
249.78	71.5	3.8402	5.19	0.03	0.80307	324.24
249.78	71.2	2.7917	-2.57	-0.09	0.80303	254.91
249.78	71.2	1.8057	-13.27	-0.67	0.80303	179.85
249.76	71.4	1.4990	-16.61	0.11	0.803081	52.72

Table I. Continued

t °C	p bars	m mol-kg^{-1}	V_ϕ cm^3-mol^{-1}	δV_ϕ	ρ_0[a] g-cm^{-3}	$10^3\delta\rho$
249.78	71.3	1.4990	-16.45	0.28	0.80304	152.53
249.76	71.6	0.9867	-25.47	-0.07	0.80311	106.31
249.79	71.3	0.7354	-30.33	0.67	0.80303	81.39
249.76	71.5	0.4873	-37.55	0.40	0.80310	56.06
249.76	71.4	0.2421	-47.69	0.31	0.80308	29.30
249.78	407.0	6.1500	21.89	0.15	0.83530	428.10
249.78	407.0	4.9516	17.63	-0.12	0.83530	371.09
249.78	407.0	3.8317	12.73	-0.08	0.83530	308.63
249.79	405.0	2.7827	6.97	0.40	0.83512	240.51
249.78	407.0	1.7982	-1.20	0.05	0.83530	168.52
249.79	406.0	1.4990	-4.47	-0.20	0.83520	144.44
249.79	408.0	0.9857	-10.44	-0.15	0.83537	99.43
249.78	407.0	0.8723	-11.68	0.20	0.83530	88.73
249.80	407.0	0.7344	-13.51	0.42	0.83527	75.63
249.80	407.0	0.4863	-19.30	-1.19	0.83527	52.04
249.80	405.0	0.2416	-24.20	-0.60	0.83511	26.6

[a] From the equation of state of Haar, Gallagher, and Kell, Ref. 15.

Table II. Parameters for Eqs. (5-7)

Parameter	V_ϕ^o	$10^5\beta^{(0)V}$	$10^4\beta^{(1)V}$	10^6C^V
a_1	-55.4270	37.7288	5.55018	-51.5161
a_2	0	0	0	4164.87
a_3	0.461152	-0.174685	0	0.176454
10^4a_4	-7.19765	3.06027	0	-2.27667
a_5	98.0419	0	0	0
a_6	8897.98	-4017.48	-1812.48	1751.07
10^2b_1	0	8.09817	0	0.181875
b_2	0	-0.0148704	0	0
b_3	0	-0.232637	0	-0.0533035
b_4	0	2.36509	0	-0.456872
c_1	0	0	0	0
c_2	-2085.48	0	0	0

Table III. Coefficients for Eqs. (9-11)

i	d	e	f
1	-5.2034×10^{-5}	-1.6060×10^{-6}	2.2983×10^{-9}
2	2.3218×10^{-7}	-1.0039×10^{-4}	1.1729×10^{-7}
3	1.9253×10^{-3}	6.7365×10^{-6}	-9.7004×10^{-9}
4	6.2883×10^{-7}	6.0370×10^{-9}	-8.4041×10^{-12}
5	1.4156×10^{-4}	-3.3880×10^{-12}	4.7899×10^{-15}

where $\alpha = 2.0$ kg$^{1/2}$ -mol$^{-1/2}$. V_ϕ^∞, $\beta^{(0)V}$, and C^V were assumed to be dependent on temperature and pressure while $\beta^{(1)V}$ was found to be independent of pressure. Simonson *et al.*[2] demonstrated that the compressibility coefficient for water $\beta_T = -(1/V)(\partial V/\partial p)_T$ can be used to represent the nonlinear behavior of V_ϕ with respect to pressure with a minimum number of adjustable parameters; this representation has again been adopted here. A generalized expression for the temperature (T, K) and pressure (p, bars) dependence of the parameters is given by

$$Q(T,p) = q_1(T) + pq_2(T) + \beta_T q_3(T) \tag{4}$$

where

$$q_1(T) = a_1 + a_2/T + a_3T + a_4T^2 + a_5/(T-227) + a_6/(647-T) \tag{5}$$

$$q_2(T) = b_1 + b_2\ln T + b_3/(T-227) + b_4/(647-T) \tag{6}$$

$$q_3(T) = c_1 + c_2T \tag{7}$$

A total of 24 adjustable parameters a_i, b_i, and c_i were used to represent the experimental results; values of these parameters are given in Table II. While 647 and 227 K represent singularity points for H_2O the terms $(T\text{-}227)^{-1}$ and $(647\text{-}T)^{-1}$ are only intended to give Eq. (4) the necessary flexibility to fit the data as opposed to the alternative of including higher order polynomial terms in Eqs. (5-6).

While β_T may readily be obtained from the equation of state for water of Hill,[19] for convenience this quantity may also be expressed to 250°C as a simple function of temperature and pressure:

$$\beta_T = \beta_T^s + (p-p_s)k_1(T) + (p-p_s)^2k_2(T) \tag{8}$$

The compressibility along the saturation vapor pressure curve β_T^s is given by:

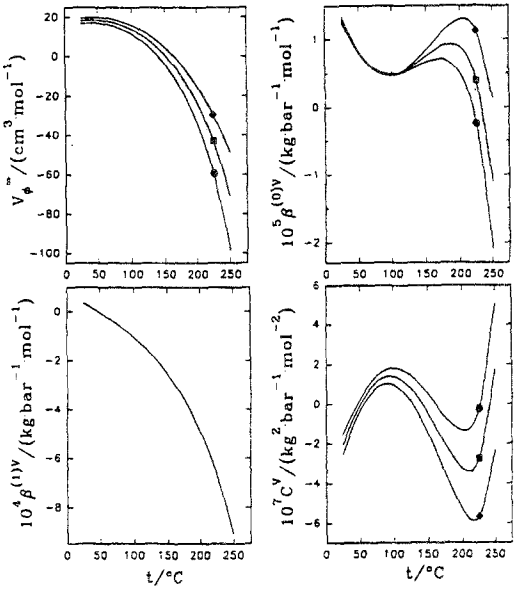

Fig. 1. Fit parameters V_ϕ°, $\beta^{(0)V}$, $\beta^{(1)V}$, and C^V plotted against temperature at •, p_0, □, 200 and ♦, 400 bars.

$$\beta_T^s = d_1 + d_2T + d_3/(T-227) + p_s[d_4 + d_5/(647-T)] \quad (9)$$

where p_0 is the saturation vapor pressure of water in bars (note p_0=1 bar for $t \leq 100$°C) and β_T^s has units of bar^{-1}. The other temperature dependent functions of Eq. (8) are

$$k_1(T) = e_1 + e_2/(647-T) + e_3\exp(-1000/[647-T]) + e_4T + e_5T^2 \quad (10)$$

$$k_2(T) = f_1 + f_2/(647-T) + f_3\exp(-1000/[647-T])) + f_4T + f_5T^2 \quad (11)$$

The coefficients listed in Table III for Eqs. (9-11) were produced by fitting these equations to values of β_T from Hill.[19]

Figure 1 shows V_ϕ°, $\beta^{(0)V}$, and C^V as functions of temperature at p_0, 200, and 400 bars. $\beta^{(1)V}$ is also shown but is independent of pressure. V_ϕ° is the only parameter which is nonlinear in pressure; its pressure dependence at 25 to 250°C is shown in Fig. 2. The nonlinearity of V_ϕ° with pressure is discernible at 200°C and is obvious at 250°C. Smoothed values of V_ϕ calculated from Eq. (2) at round values of molality and at p_0, 200, and 400 bars are presented in Table IV. Errors in the measured relative densities were calculated according to:

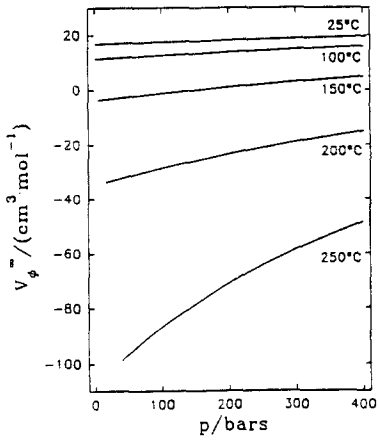

Fig. 2. V_ϕ° plotted as a function of pressure along 25 to 250°C isotherms.

$$\delta\rho_\pm = \left[\frac{\delta\tau_{err}^2}{\delta\tau^2} + \frac{\kappa_{err}}{\kappa}\right]\delta\rho \qquad (12)$$

where τ is the instrument's period of vibration and κ is a proportionality constant characteristic of the vibrating tube at a given temperature and pressure. Errors in the densities of the calibrating fluids have been ignored and as a consequence the errors in $\delta\rho$ are understated; however, $\delta\rho_\pm$ is appropriate for interlaboratory comparison. Errors were found to be independent of pressure but increase with temperature as shown in Table V.

4. DISCUSSION

Though the fit of V_ϕ for $CaCl_2$(aq) requires the inclusion of an ionic strength dependence in the second virial coefficient, and several more parameters to represent the temperature- and pressure-dependence of the molality-independent coefficients, there are notable similarities between the terms used to fit V_ϕ for both NaCl(aq) and $CaCl_2$(aq). $V_\phi^\circ(CaCl_2)$ has the same qualitative behavior with temperature characteristic of most electrolytes, with a broad maximum in V_ϕ° below 100°C and a steep decrease at higher temperatures. The maximum value of $V_\phi^\circ(CaCl_2)$ is found at somewhat lower temperatures than for V_ϕ°(NaCl) (about 35°C versus about 65°C at p_0); however the magnitudes at p_0 and 400 bars are comparable at about 18 and 20 cm^3-mol^{-1}, respectively. At higher temperatures $V_\phi^\circ(CaCl_2)$ falls off more rapidly reaching -99 and -49 at 250°C and p_0 and 400 bars, respectively, versus -30 and -10 for

Table IV. Calculated Apparent Molar Volumes for $CaCl_2$(aq)

°C	Molality m 0.0	0.10	0.25	0.50	0.75	1.0	2.0	3.0	4.0	5.0	6.0
					$p = p_0$ [a]						
25	16.83	19.45	20.73	22.04	22.99	23.77	26.19	28.08	29.72	31.18	32.51
50	17.14	20.19	21.52	22.86	23.82	24.60	26.96	28.79	30.40	31.88	33.28
75	15.32	19.00	20.49	21.96	23.01	23.86	26.42	28.41	30.17	31.82	33.42
100	11.43	16.03	17.77	19.49	20.73	21.75	24.81	27.18	29.25	31.19	33.07
125	5.28	11.20	13.35	15.48	17.03	18.31	22.20	25.16	27.69	30.00	32.19
150	-3.61	4.24	7.00	9.75	11.77	13.45	18.51	22.28	25.41	28.15	30.65
175	-16.10	-5.33	-1.64	2.03	4.72	6.95	13.60	18.40	22.24	25.48	28.29
200	-33.74	-18.45	-13.30	-8.27	-4.61	-1.62	7.12	13.21	17.90	21.69	24.85
225	-59.39	-36.72	-29.18	-21.99	-16.90	-12.80	-1.22	6.49	12.23	16.75	20.44
250	-98.61	-63.03	-51.30	-40.45	-33.02	-27.19	-11.44	-1.46	5.79	11.51	16.31
					p = 200 bars						
25	18.22	20.75	21.99	23.25	24.17	24.93	27.23	29.00	30.51	31.82	32.99
50	18.66	21.55	22.83	24.11	25.02	25.77	28.02	29.76	31.27	32.66	33.95
75	17.18	20.60	21.98	23.34	24.32	25.12	27.52	29.39	31.03	32.55	34.02
100	13.85	18.03	19.60	21.16	22.28	23.21	26.03	28.21	30.11	31.86	33.55
125	8.56	13.82	15.69	17.57	18.96	20.12	23.65	26.35	28.64	30.70	32.62
150	1.03	7.83	10.17	12.53	14.31	15.80	20.38	23.80	26.62	29.05	31.21
175	-9.30	-0.24	2.78	5.85	8.17	10.13	16.10	20.46	23.92	26.76	29.15
200	-23.36	-10.93	-6.89	-2.82	0.24	2.81	10.54	16.03	20.23	23.56	26.21
225	-42.82	-25.12	-19.51	-14.00	-9.93	-6.56	3.35	10.14	15.20	9.11	22.18
250	-70.89	-44.49	-36.34	-28.63	-23.12	-18.66	-6.09	2.19	8.25	12.99	16.86
					p = 400 bars						
25	19.49	21.95	23.15	24.37	25.26	25.99	28.18	29.84	31.21	32.39	3.39
50	20.04	22.80	24.01	25.24	26.11	26.83	28.99	30.64	32.07	33.36	34.56
75	18.82	22.02	23.30	24.58	25.50	26.25	28.51	30.26	31.79	33.20	34.55
100	15.94	19.77	21.20	22.61	23.65	24.51	27.11	29.12	30.85	32.44	33.95
125	11.36	16.07	17.72	19.40	20.65	21.70	24.94	27.41	29v.48	31.31	32.99
150	4.90	10.85	12.85	14.92	16.50	17.85	22.04	25.18	27.73	29.87	31.72
175	-3.72	3.98	6.48	9.10	11.14	12.89	18.37	22.40	25.55	28.07	30.10
200	-14.95	-4.75	-1.55	1.80	4.43	6.70	13.77	18.88	22.76	25.74	27.99
225	-29.55	-15.69	-11.53	-7.23	-3.87	-0.98	7.92	14.24	18.94	22.49	25.12
250	-48.64	-29.26	-23.76	-18.28	-14.07	-10.50	0.28	7.78	13.37	17.68	21.06

[a] 1 bar for $t \leq 100$°C.

V_ϕ°(NaCl). This is probably a result of greater solvent electrostriction due to the higher charge density of the Ca^{2+} ion versus the Na^+ ion.

Few investigators have reported values of V_ϕ° for $CaCl_2$(aq) at elevated temperatures and pressures. Figure 3 illustrates differences between the estimated values of V_ϕ° from this study and those of Ellis,[9] Dunn,[10] and Monnin.[5] Ellis's estimates are in excellent agreement with this study through 150°C but are substantially larger at 175 and

Table V. Upper Limits on Statistical Errors for $\delta\rho$ and V_ϕ at Each Temperature as Calculated from Eq. (12)

t °C	$10^6\delta\rho_{err}$ [b]	$V_{\phi,err}$ [a]
25	170	0.1
50	200[c]	0.3
100	200[d]	0.4
150	250	0.4
200	300	0.4
250	400	0.6

[a] Errors in V_ϕ are inversely proportional to m so that the largest statical errors occur at the lowest molalities; errors at the highest molalities are substantially lower than those listed. Note that values for $\delta V_{\phi,\,err}$ are similar to the maximum fit deviations at each experimental temperature listed in Table I. [b] $\delta\rho_{err} = \delta\rho \pm/\rho_{soln}$. [c] Except for 300 ppm at 2.7917m. [d] Except for 1200 ppm at 3.8402m and 650 ppm at 4.9573m

200°C. Monnin's values are based on his assessment of the available density measurements treated with the ion-interaction model, and rely heavily on the results of Gates and Wood.[6,7] For $\tau \leq 125$°C all of the V_ϕ^o values are in reasonable agreement (± 2 cm^3-mol^{-1}) with our estimates. Above 125°C Monnin's values rapidly diverge from our estimates and the differences are opposite in sign to the difference between our estimates and those of Ellis. These differences are due to the differences between our experimental results and those of Gates and Wood[7] (discussed below) and to the use of different sets of molality-independent parameters in the ion-interaction model. Monnin's[4,5,20] fits of $CaCl_2$(aq) have included only $\beta^{(0)V}$ and C^V whereas $\beta^{(1)V}$ was used in this study to fit V_ϕ at the level of estimated experimental uncertainty. The fact that Gates and Wood[7] did not make measurements between 175 and 275°C may be another cause of the variance. Given the rapid change in V_ϕ^o at higher temperatures the lack of agreement with Monnin at $t \geq 125$°C is not surprising.

The inclusion of $\beta^{(1)V}$ for $CaCl_2$(aq) contrasts with our fit[2] of V_ϕ for NaCl(aq) in which only the $\beta^{(0)V}$ parameter appears in the second virial coefficient. The inclusion of $\beta^{(1)V}$ is consistant with our earlier fit of V_ϕ for $CaCl_2$(aq) at 25 and 35°C and 1 bar,[1] where a fourth virial coefficient D^V was also included. It was found that the present results are of lower precision than our previous measurements at 1 bar and that the use of the D^V parameter was not supported by the data at higher temperatures and pressures. A slight misfit of our earlier results at 25 and

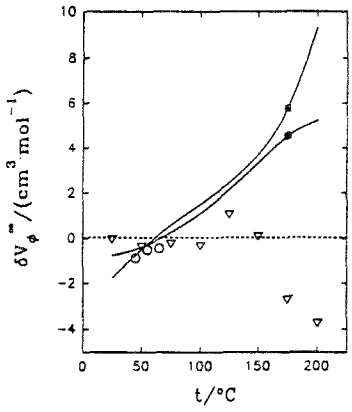

Fig. 3. Differences (δV_ϕ°) between V_ϕ° calculated from Eq. (4) and values estimated from earlier studies. O, Dunn Ref. 10, 1 bar; ∇, Ellis(9), 20 bars; • , Monnin Ref. 5, p_0; □, Monnin(5), 400 bars.

35°C and 1 bar was accepted in order to avoid overfitting of the results at higher temperatures. The inclusion of $\beta^{(1)V}$ is also consistent with previous ion-interaction treatments of $CaCl_2$ activity and osmotic coefficients.[21-24]

It is of interest to note that the behavior of V_ϕ at high molalities is not as complex as that of the excess free energy quantities ($\gamma_\pm$ and ϕ) as described by Phutela and Pitzer,[22] who found that $\gamma_\pm$ and ϕ may be represented accurately only through about 4.5 mol-kg^{-1} if the ion interaction equations are truncated at C^ϕ. Ananthaswamy and Atkinson's[23] fit of $\gamma_\pm(CaCl_2)$ using the Pitzer ion-interaction model required six molality independent parameters, including terms through m^6, to represent $\gamma_\pm$ at 1 bar to 100°C and 9.0 mol-kg^{-1}. It is clear from the results of this study that terms of higher order than C^V are unnecessary to respresent V_ϕ for $CaCl_2$(aq), implying that higher order parameters of the ion interaction treatment used to reproduce $\gamma_\pm$ or ϕ should be independent of pressure.

The form of Eq. (3) dictates that the largest contribution of the $\beta^{(1)V}$ term occurs at low ionic strengths. Comparison of Fig. 1 with Fig. 4, however, shows that due to the relative magnitudes of $\beta^{(0)V}$ and $\beta^{(1)V}$ the second term in Eq. (3) contributes significantly to B^V over wide ranges of temperature and ionic strength. Thus, while $\beta^{(1)V}$, in principle, is intended to represent the change in B^V with ionic strength at low molalities, where only precise density measurements warrant the use of $\beta^{(1)V}$ due to the dependence of V_ϕ on ρ and m; $\beta^{(1)V}$ does have a finite

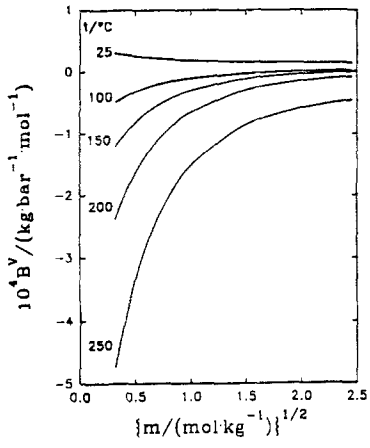

Fig. 4. Values of B^V from Eq. (3), plotted against $\sqrt{m}$ at p_0.

value at high molalities, which remains weakly dependent on ionic strength, and therefore contributes to the fit over the entire molality range. It must be stressed that in our model all parameters other than the A_V coefficient in the Debye-Hückel term are empirical fit parameters and as such are not meant to individually describe particular properties of the solution or solute species interactions.

The temperature-dependent forms of $\beta^{(0)V}$ and C^V are similar to the corresponding terms for NaCl(aq)[2] in that both coefficients have sigmoidal forms, with rapidly increasing absolute values for $(\partial\beta^{(0)V}/\partial T)_p$ and $(\partial C^V/\partial T)_p$ at the low and high temperature extremes and an inflection point near 150°C in each case. For both $CaCl_2$(aq) and NaCl(aq) $\beta^{(0)V}$ decreases strongly with increasing temperature at the low and high temperature extremes considered here, while the temperature dependence of C^V shows the opposite behavior. The weak dependence of $\beta^{(0)V}(CaCl_2)$ on pressure below 125°C and increasing pressure dependence at higher temperatures is qualitiatively similar to the behavior observed for $\beta^{(0)V}$(NaCl) by Rogers and Pitzer.[18] Our $\beta^{(0)V}(NaCl)$[2] had a very weak pressure dependence over the entire 25-250°C range. The other important distinction between the fitting parameters for NaCl and $CaCl_2$ is that there is a pressure dependence on $C^V(CaCl_2)$ which also increases with increasing temperature. It is likely that some covariance of $\beta^{(0)V}$ and C^V in their contribution to V_ϕ leads to this partially compensating variation in their temperature dependences. It is clear from inspection of the rapid changes of these parameters with temperature at the upper and lower ends of the temperature range of the present

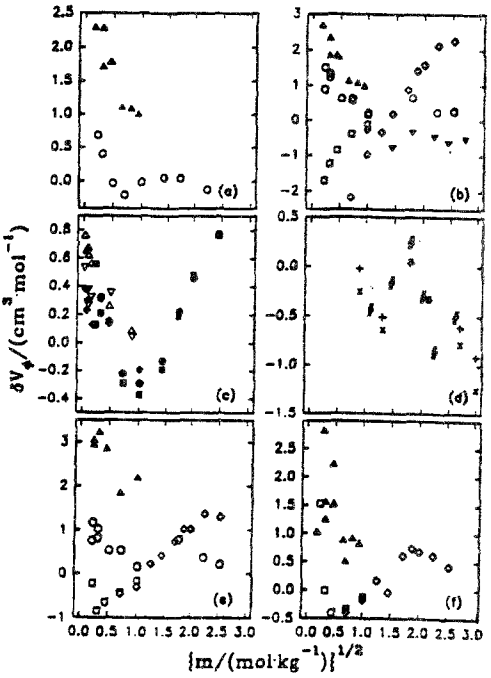

Fig. 5. δV_ϕ plotted *vs.* $\sqrt{m}$ for temperatures to 100°C at low pressures. (a) 25°C: O, Ref. (6); Δ, Ref. (12). (b) 50°C: O, Ref. (7); Δ, Ref. (12); □ Ref. (9); ♦ Ref. (11); ∇ Ref. (8). (c) From Ref. (13) at • 45°C and □, 55°C; from Ref. (10) at ∇, 45°C, 55°C, ♦ 65°C. (d) From Ref.(8) at + 60°C, × 70°C, # 80°C. (e) 75°C: O, Ref. (7); Δ, Ref. (12); □ Ref. (9), ♦ Ref. (11). (f) 100°C: Δ, Ref. (12); □ Ref. (9); ♦ Ref. (11).

measurements that extrapolation of the fit equations beyond the range of experimental results is unlikely to give satisfactory results.

Differences (δV_ϕ) between V_ϕ values calculated from Eq. (2) and previously reported V_ϕ values[6-13] are shown in Figs. 5-7. V_ϕ values presented in the original texts were used directly where available; published values of ρ or δρ were converted to V_ϕ using the Hill[19] equation of state for water. The δρ data of Gates and Wood[6,7] were converted to V_ϕ using the Haar *et al.*[15] equation of state for water to maintain consistency with the water density values used in the original work. Ellis's[9] data are always within 1500 ppm in density of our calculated V_ϕ data and are relatively well dispersed around our values. Kumar[11] also reported measurements at 20 bars, 50 to 200°C, and for molalities which overlap with Ellis's high molality (0.5 and 1.0 mol-kg^{-1}) measurements and extend to 6.4 mol-kg^{-1}. Kumar's data appear to have low internal

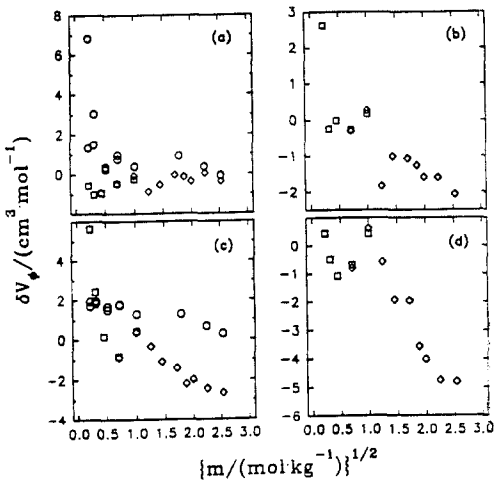

Fig. 6. δV_ϕ plotted against $\sqrt{m}$ for temperatures from 125 to 200°C at low pressures. Symbols: Ref. O, (7); □ Ref. (9); ♦ Ref. (11). Graphs: (a) 125°C; (b) 150°C; (c) 175°C; (d) 200°C.

precision, though his two lowest molality V_ϕ values are generally in remarkably good agreement with Ellis's data. Kumar's V_ϕ values are generally larger than those calculated from Eq. (2) below 100°C, are in good agreement at 125°C, and are substantially lower for ionic strengths greater than 2.0 mol-kg^{-1} at and above 150°C. Though the V_ϕ measurements from Gates and Wood[7] are in better agreement with our data, their values are almost always larger than our calculated values at temperatures and pressures above 50°C and 1 bar, and at 125 and 175°C are often outside of our estimated error limits. The larger differences observed for their 6.4 mol-kg^{-1} data are due to errors in extrapolating beyond the range of our highest molality samples using Eq. (2).

It is possible that the differences between our results and those of Gates and Wood[7] above 100°C were due to corrosion of our vibrating tube at $t \leq 200$°C; however, we observed no indications that the tube was corroding below 250°C. In addition, many of our NaCl(aq) V_ϕ measurements[2] were made contemporaneously with the $CaCl_2$(aq) measurements, and the V_ϕNaCl(aq) compared well with those of Majer *et al.*[25] through 225°C.

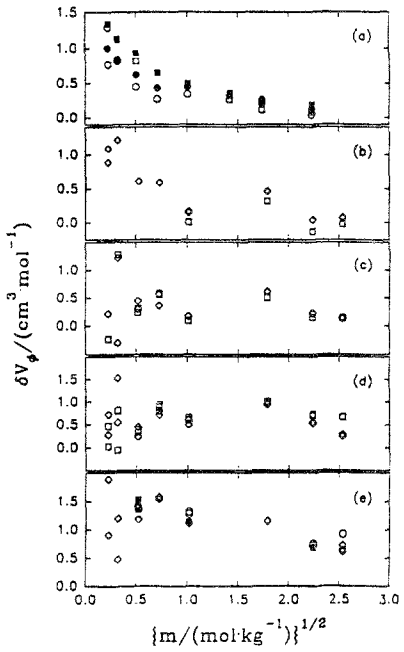

Fig. 7. δV_ϕ plotted against$\sqrt{m}$ for temperatures from 25 to 175°C at high pressures. (a) From Ref. (6) at 25°C and O, 103 bars, • 171 bars, □, 312 bars, □ 405 bars. (b-e) From ref. (7). Symbols: ♦ 203 bars; □, 290 bars; □ 400 bars. Graphs: (b) 50°C, (c) 75°C, (d) 125°C, (e) 175°C.

5. ACTIVITY COEFFICIENTS AT ELEVATED PRESSURES AND TEMPERATURES

One of the important uses of volumetric data for electrolyte solutions is in the calculation of the pressure dependence of other thermodynamic properties, *e.g.*, activity and osmotic coefficients. In the Pitzer ion-interaction formalism the coefficients A_V, B^V, and C^V are the pressure derivatives of the respective virial coefficients for the excess Gibbs free energy:

$$A_V = (\partial A_\phi/\partial p)_T \tag{13}$$

$$B^V = (\partial B/\partial p)_T \tag{14}$$

$$C^V = (\partial C/\partial p)_T = (\partial C^\phi/\partial p)_T/2\,|\,z_M z_X\,|^{1/2} \tag{15}$$

Thus if the parameters A_ϕ, B, and C^ϕ have been determined at a set

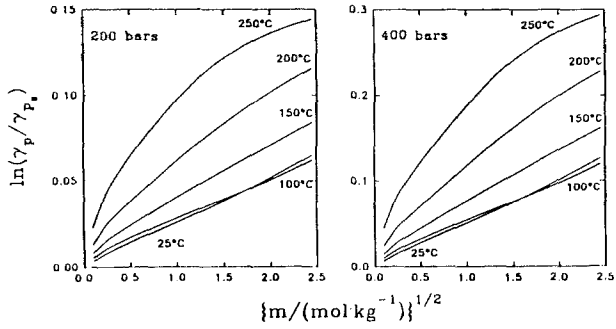

Fig. 8. The quantities (a) $\ln[\gamma_{\pm}(200\ \text{bars})/\gamma_{\pm}(p_0)]$ and (b) $\ln[\gamma_{\pm}(400\text{bars})/\gamma_{\pm}(p_0)]$ plotted *vs.* $\sqrt{m}$ at various temperatures.

of reference temperatures and pressures the volumetric parameters in Eq. (2) can be integrated to yield activity coefficients at pressures to 400 bars. Phutela and Pitzer,[22] Ananthaswamy and Atkinson,[23] and Møller[24] have fitted values of $\gamma_{\pm}$ and ϕ for $CaCl_2$(aq) near the saturation vapor pressure to temperature dependent forms of the ion-interaction model, and these quantities can be used as reference values, in conjunction with the representation for volumetric properties presented here, to calculate $\gamma_{\pm}$ or ϕ at pressures to 400 bars and temperatures to 250°C. As a more complete treatment of the thermodynamic properties of $CaCl_2$(aq) was published while this paper was in preparation,[26] we will not present here extensive calculations of $CaCl_2$(aq) thermodynamics at higher pressures, but will show as an example the pressure dependence of $\gamma_{\pm}$ as a function of temperature and molality over the ranges addressed in this work.

The ion interaction expression for the pressure dependence of the mean ionic activity coefficient, written specifically for a 2-1 charge-type electrolyte, is

$$\ln[\gamma_{\pm}(p)/\gamma_{\pm}(p_o)] = -2[A_{\phi}(p) - A_{\phi}(p_o)]\left[\frac{\sqrt{I}}{1+b\sqrt{I}} + (2/b)\ln(1+b\sqrt{I})\right]$$

$$+ (4/3)m\int_{p_0}^{p}\left(2\beta^{(0)V} + 2\beta^{(1)V}[1 - (1+\alpha\sqrt{I}-\alpha^2 I/2)\exp(-\alpha\sqrt{I})]\alpha^2 I + 3mC^{V}\right)dp \tag{16}$$

Integration of the general temperature and pressure dependence Eq. (4) for the ion interaction parameters is straightforward, and gives

$$Z(T,p)\int_{p_0}^{p} Q(T,p)\mathrm{d}p = (p-p_0)q_1(T) + (p_1^2-p_0^2)q_2(T)/2+\ln[\rho(p)/(p_0)]q_3(T) \quad (17)$$

Figure 8 shows plots of $\ln[\gamma_\pm(p)/\gamma_\pm(p_0)]$ for p = 200 and 400 bars, versus the square root of the molality for temperatures from 25 to 250°C. The effect of pressure on $\ln\gamma_\pm$ is very small at low ionic strengths but becomes progressively larger with increasing molality and temperature. It should be noted that the calculated differences are nearly linear with pressure at these relatively high pressures; that is, $\ln[\gamma_\pm(400 \text{ bars})/\gamma_\pm(p_0)] \approx 2\ln[\gamma_\pm(200 \text{ bars})/\gamma_\pm(p_0)]$. Also, the relatively small changes in $\gamma_\pm$ with pressure are very weak functions of temperature from 25 to 100°C. The effect of the nonlinearity of A_ϕ with pressure is significant only at pressures below 200 bars.

ACKNOWLEDGMENT

The research at VPI was sponsored by the Division of Engineering and Geosciences Office of Basic Energy Sciences, U. S. Dept. of Energy under grant DE-FG05-89ER14065.

The research at ORNL was sponsored by the Division of Chemical Sciences, Office of Basic Energy Sciences, U. S. Dept. of Energy under Contract No. DE-AC05-84OR21400 with Martin Marietta Energy Systems, Inc.

REFERENCES

1. C. S. Oakes, J. M. Simonson, and R. J. Bodnar, *J. Chem. Eng. Data* **35**, 304 (1990).
2. J. M. Simonson, C. S. Oakes, and R. J. Bodnar, *J. Chem. Thermodyn.* **26**, 345 (1994).
3. K. S. Pitzer, *J. Phys. Chem.* **77**, 268 (1973).
4. C. Monnin, *J. Solution Chem.* **16**, 1035 (1987).
5. C. Monnin, *Geochim. Cosmochim. Acta* **54**, 3265 (1990).
6. J. A. Gates and R. H. Wood, *J. Chem. Eng. Data* **30**, 44, (1985).
7. J. A. Gates and R. H. Wood, *J. Chem. Eng. Data* **34**, 53 (1989).
8. E. P. Perman and W. D. Urry, *Proc. Royal Soc. London (A)* **126**, 44, (1930).
9. A. J. Ellis, *J. Chem. Soc. (A)* 660 (1967).
10. L. A. Dunn, *Trans. Faraday Soc.* **64**, 2951 (1968).
11. A. Kumar, *J. Solution Chem.* **15**, 409 (1986).
12. P. P. S. Saluja and J. C. LeBlanc, *J. Chem. Eng. Data* **32**, 72 (1987).
13. T. Isono, *J. Chem. Eng. Data* **29**, 45 (1984).
14. C. S. Oakes, J. M. Simonson, and R. J. Bodnar, *Geochim. Cosmochim. Acta* **54**, 603, (1991).
15. L. Haar, J. S. Gallagher, and G. S. Kell, *NBS/NRS Steam Tables*, (Hemisphere: Washington DC, 1984).

16. P. S. Z. Rogers and K. S. Pitzer, *J. Phys. Chem. Ref. Data* **11**, 15 (1982).
17. D. J. Bradley and K. S. Pitzer, *J. Phys. Chem.* **83**, 1599 (1979).
18. D. G. Archer and P. Wang, *J. Phys. Chem. Ref. Data* **19**, 371 (1990).
19. P. G. Hill, *J. Phys. Chem. Ref. Data* **19**, 1233 (1990).
20. C. Monnin, *Geochim. Cosmochim. Acta* **53**, 1177 (1989).
21. H. F. Holmes, C. F. Baes, Jr., and R. E. Mesmer, *J. Chem. Thermodyn.* **10**, 983 (1978).
22. R. C. Phutela and K. S. Pitzer, *J. Solution Chem.* **12**, 201, (1983).
23. J. Ananthaswamy and G. Atkinson, *J. Chem. Eng. Data* **30**, 120, (1985).
24. N. Møller, *Geochim. Cosmochim. Acta* **52**, 821 (1988).
25. V. Majer, J. A. Gates, A. Inglese, and R. H. Wood, *J. Chem. Thermodyn.* **20**, 949, (1988).
26. H. F. Holmes, R. H. Busey, J. M. Simonson, and R. E. Mesmer, *J. Chem.* Thermodyn. **26**, 271, (1994).